Orthogonal Transformation Based Robust Adaptive Close Formation Control of Multi-UAVs

Y. D. Song, *Member, IEEE*, Yao Li, *Student Member, IEEE* and X. H. Liao

Abstract— **Traditional coordination control of UAVs has been developed mainly based on linear models, giving local results. This paper presents an orthogonal transformation-based robust adaptive control method for close formation flight of multi-UAVs, and the result is global. Uncertain dynamics and disturbances due to vortex are explicitly addressed in control design. The overall control scheme proposed herein has simple structure and does not demand detail system dynamic information. There is no need to re-design and reprogram the control strategy even when flight condition changes. Simulation verification is included.**

I. Introduction

Recent years have witnessed an increasing interest in research and application of Unmanned Aerial Vehicles (UAVs) [1-12]. The requirement to coordinate multi-UAVs continues to surface in both defense and civil applications. The realization of operating a group of mutli-UAVs in close formation as gracefully as the flock of birds (e.g., Figure 1) relies on many enabling technologies, among which advanced control methodologies are imperative. Various control schemes for formation flight have been reported. Early contributors on close formation control include Blake and Multhopp [1], D'Azzo and his coworkers [2], Bozugany and Pachter [3], Fierro et al. [4], Giulitti et al [5], Jongusuk et al [6], Reyna and Pachter [7], Richards et al [8], and Wolfe et al [9]. Most of the results are based on flight models that either linearize the nonlinear flight dynamics and/or ignore the effect of vortex. Singh [10] and Schumacher et al [11] considered the nonlinear property of vortex and studied the control problem using backstepping design method. In the recent work by Song et al [12], nonlinear model with uncertain dynamics arising from close formation was explicitly addressed.

This paper extends the result of [12] to deal with more general case of uncertain dynamics due to vortex and external disturbances. Robust and adaptive control algorithms capable of maintaining desirable separation of wingman with the leading UAV are developed. Compared with most existing methods, the formation control scheme presented in this paper is simpler in structure and easier to implement.

Fig. 1. Formation flight of flock of birds and aerial vehicles

II. Dynamic Model and Problem Formulation

The formation geometry is determined by the relative position between the Leader and Wingman as shown in Figure 2. The formation control objective is to steer the Wingman (follower) to maintain certain separation distance in longitudinal, lateral and vertical directions. By properly defining the body frame and inertia frame, the following three equations describing dynamic behavior of wingman aircraft can be established

$$\dot{V}_w = g_v(.)u_v + \Delta f_v(\bullet) \tag{1}$$

$$\ddot{\psi}_w = g_\psi(.)u_\psi + \Delta f_\psi(\bullet) \tag{2}$$

$$\ddot{h}_w = g_h(.)u_h + \Delta f_h(\bullet) \tag{3}$$

with

$$\Delta f_v(\bullet) = \frac{\bar{q}s}{m}\Delta c_{Dw_y}(y - y_d) + \delta_1(.) \tag{4}$$

$$\Delta f_\psi(\bullet) = \frac{\bar{q}s}{mV_w}[\Delta c_{Iw_y}(y - y_d) + \Delta c_{Iw_h}(h - h_d)] + \delta_2(.) \tag{5}$$

$$\Delta f_h(\bullet) = \frac{\bar{q}s}{m}\Delta c_{Lw_y}(y - y_d) + \delta_3(.) \tag{6}$$

where V_w, ψ_w and h denote the wingman's heading velocity, heading angle and altitude, $g_v(.)$, $g_\psi(.)$ and $g_h(.)$ are system control gains, u_v, u_ψ and u_h are the control inputs. The effect of vortex are represented by $\Delta f_v(\bullet)$, $\Delta f_\psi(\bullet)$ and $\Delta f_h(\bullet)$, in which s is wing area, m is gross mass, $\bar{q}$ is dynamic

Manuscript received September 14, 2004. This work was supported in part funding provided by ONR through the grant N00014-03-1-0462.

Y. D. Song and X. H. Liao are with the North Carolina A&T State University, Greensboro, NC 27411 USA (phone: 336-334-7760; fax: 336-334-7716; e-mail: songyd@ ncat.edu).

Yao Li was with the North Carolina A&T State University, Greensboro, NC 27411 USA. He is now with the Department of Electrical & Computer Engineering University of Maryland, College Park, MD 20742 USA, (e-mail: yaoli@umd.edu).

pressure, Δc_{DW} is drag coefficient, Δc_{IW} is side-wash coefficient, Δc_{LW} is lift coefficient, and $\delta_i(.)$'s are lumped uncertain system dynamics and external disturbances. Compared with most flight dynamic models used in UAVs studies (i.e. [1]-[14]), the model considered here is more effective in reflecting the nonlinear dynamic behaviors of UAVs.

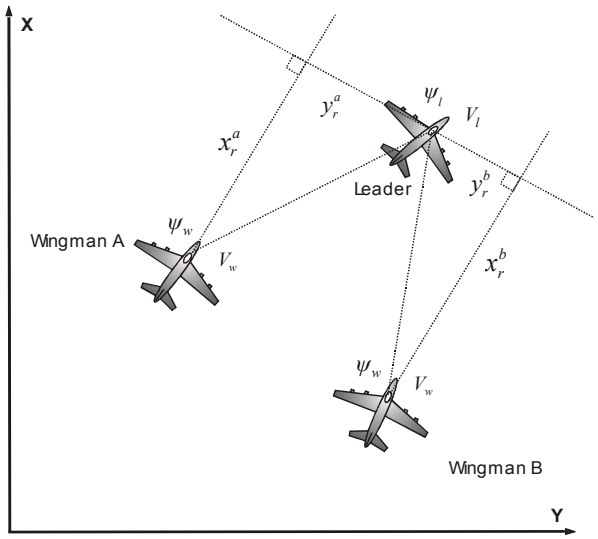

Fig. 2. Multi-UAVs in close formation flight

The definitions of the variables and the subscripts of the variables used in this paper and are listed in Table I and Table II respectively.

TABLE I
NOMENCLATURE OF THE VARIABLES

Parameter	Variable
Aircraft Mass	m
Dynamic Pressure	$\overline{q}$
Wing Area	s
Distance of X Coordinate	x
Distance of Y Coordinate	y
Altitude	h
Heading Velocity	V
Heading Angle	ψ
Autopilot Time Constant	τ

One of the important tasks in close formation is to separate the wingman away from the leading UAV with certain distance in lateral (x-axis), longitudinal (y-axis) and vertical (h-axis) directions to prevent possible collision. To address this issue, a relative frame as shown in Figure 2 is considered. The relative coordinates are defined by

$$x_r = x_l - x_w,\ y_r = y_l - y_w \text{ and } h_r = h_l - h_w.$$

TABLE II
SUBSCRIPTS OF THE VARIABLES

Parameter	Subscript
Desired Value	d
Separation / Difference	e
Control Signal	c
Leader Aircraft	l
Wingman Aircraft	w
Drag Coefficient	D
Side-wash Coefficient	I
Lift Coefficient	L
Relative measurement	r

The formation control problem can be stated as follows: *Design control algorithms to maintain the wingman's relative position* (x_r, y_r, h_r) *at the desired value with respect to the leader aircraft.* Namely, the heading velocity control u_v, heading angle control u_ψ, and altitude control u_h are to be designed so that

$$x_r = x_l - x_w \to x_d \tag{7}$$

$$y_r = y_l - y_w \to y_d \tag{8}$$

$$h_r = h_l - h_w \to h_d \tag{9}$$

where x_d, y_d and h_d are the desired formation distance in x, y and h coordinates.

III. ROBUST AND ADAPTIVE CONTROL DESIGN

In view of the relative coordinate frame as illustrated in Figure 2, we derive the following relative kinematics equations,

$$\dot{x}_r = V_l \cos(\psi_l - \psi_w) + \dot{\psi}_w y_r - V_w \tag{10}$$

$$\dot{y}_r = V_l \sin(\psi_l - \psi_w) - \dot{\psi}_w x_r \tag{11}$$

$$\dot{h}_r = \dot{h}_l - \dot{h}_w \tag{12}$$

Upon introducing the separation error

$$e_x = x_r - x_d \tag{13}$$

$$e_y = y_r - y_d \tag{14}$$

$$e_h = h_r - h_d \tag{15}$$

and making use of the relative kinematics equations (9)-(12), we can express the lateral, longitudinal and vertical formation error dynamics as

$$\begin{bmatrix} \dot{e}_x \\ \dot{e}_y \\ \dot{e}_h \end{bmatrix} = A(\psi_l, \psi_w) + R(x_r, y_r) \begin{bmatrix} V_w \\ \dot{\psi}_w \\ \dot{h}_w \end{bmatrix} \tag{16}$$

where

$$A(\psi_l,\psi_w)=\begin{bmatrix} V_l\cos(\psi_l-\psi_w) \\ V_l\sin(\psi_l-\psi_w) \\ \dot{h}_l \end{bmatrix}$$

$$R(x_r,y_r)=\begin{bmatrix} -1 & y_r & 0 \\ 0 & -x_r & 0 \\ 0 & 0 & -1 \end{bmatrix}$$

Note that the inverse of R is not defined at $x_r=0$ (this physically corresponds to the situation that the relative distance in x-axis from Wingman toward Leader becomes zero, which could happen anytime), direct stabilization of e_x, e_y and e_h is unfeasible. To circumvent this problem, we perform an orthogonal coordinate transformation

$$E=\begin{bmatrix} E_x \\ E_y \\ E_h \end{bmatrix}=B(\psi_w)\begin{bmatrix} e_x \\ e_y \\ e_h \end{bmatrix} \tag{17}$$

where $B(\psi_w)$ is defined as

$$B(\psi_w)=\begin{bmatrix} \sin\psi_w & \cos\psi_w & 0 \\ \cos\psi_w & -\sin\psi_w & 0 \\ 0 & 0 & 1 \end{bmatrix} \tag{18}$$

and

$$B^T(\psi_w)B(\psi_w)=\begin{bmatrix} 1 & 0 & 0 \\ 0 & 1 & 0 \\ 0 & 0 & 1 \end{bmatrix} \quad \forall\psi_w \tag{19}$$

Consequently, we have

$$\|E\|^2=\left\|\begin{matrix} e_x \\ e_y \\ e_h \end{matrix}\right\|^2 \tag{20}$$

Therefore the problem of stabilizing e_x, e_y and e_h boils down to stabilizing E_x, E_y, and E_h. Our controller design now is focused on the transformed error dynamics. From (16)-(17), we have

$$\dot{E}=BA+C\begin{bmatrix} V_w \\ \dot{\psi}_w \\ \dot{h}_w \end{bmatrix} \tag{21}$$

where

$$C=BR+\frac{\partial B}{\partial\psi_w}\begin{bmatrix} e_x \\ e_y \\ e_h \end{bmatrix}\begin{bmatrix} 0 & 1 & 0 \end{bmatrix} \tag{22}$$

Combining (21) with (1)-(3) leads to

$$\ddot{E}=CG\begin{bmatrix} u_v \\ u_\psi \\ u_h \end{bmatrix}+N+C\begin{bmatrix} \Delta f_v(.) \\ \Delta f_\psi(.) \\ \Delta f_h(.) \end{bmatrix} \tag{23}$$

where

$$N=\begin{bmatrix} \dot{V}_l\sin\psi_l+\dot{\psi}_l V_l\cos(\psi_l) \\ \dot{V}_l\cos\psi_l-\dot{\psi}_l V_l\sin(\psi_l) \\ \ddot{h}_l \end{bmatrix}+\dot{C}\begin{bmatrix} V_w \\ \dot{\psi}_w \\ \dot{h}_w \end{bmatrix} \tag{24}$$

$$G=diag(g_v,g_\psi,g_h) \tag{25}$$

Note that the matrix C as defined in (22) is always invertible because from the definition of B and R, we can show that

$$C=\begin{bmatrix} -\sin\psi_w & y_d\sin\psi_w-x_d\cos\psi_w & 0 \\ -\cos\psi_w & y_d\cos\psi_w+x_d\sin\psi_w & 0 \\ 0 & 0 & -1 \end{bmatrix}$$

which has $\det(C)=x_d$. Now we are in the position to present the first control scheme, which is based on G and N.

Theorem 1: Consider the transformed error dynamics (23), where the lumped uncertain vector satisfies

$$\left\|\begin{matrix} \Delta f_v \\ \Delta f_\psi \\ \Delta f_h \end{matrix}\right\|\triangleq\|\Delta f(.)\|\le\sum_{i=1}^{m}b_i\xi_{fi} \tag{26}$$

where $b_i\ge 0$ is unknown constant and ξ_{fi} is the known regressor. If the following robust adaptive control scheme is applied, then stable close formation of multi-UAVs is ensured,

$$\begin{bmatrix} u_v \\ u_\psi \\ u_h \end{bmatrix}=-(CG)^{-1}\left[(k_r+k_a)S-N-\beta\dot{E}\right] \tag{27}$$

with

$$S=\dot{E}+\beta E,\ \ (\beta>0) \tag{28}$$

$$k_r>0,\ k_a=\frac{\hat{a}_1\Upsilon_1}{\|S\|}$$

where

$$\Upsilon_1=\|C\|\sum_{i=1}^{m}\xi_{f_i}\ \text{ and }\ \dot{\hat{a}}_1=\|S\|\Upsilon_1 \tag{29}$$

Proof:

From (23) and (28) it follows that

$$\dot{S}=CG\begin{bmatrix} u_v \\ u_\psi \\ u_h \end{bmatrix}+N+\beta\dot{E}+C\Delta f(.)$$

It can be shown from (26) that

$$\|C\Delta f(.)\| \le a_1 \Upsilon_1$$

where $a_1 = \max\{b_1,...,b_m\}$ and Υ_1 is defined as in (29). With the control scheme (27), it is seen that

$$\dot{S} = -k_r S - k_a S + C\Delta f(.) \tag{30}$$

Consider the Lyapunov function candidate

$$V = \frac{1}{2} S^T S + \frac{1}{2}\tilde{a}_1^2 \tag{31}$$

where $\tilde{a}_1 = a_1 - \hat{a}_1$ and $\hat{a}_1$ is the estimate of a_1. It follows from (30)-(31) that

$$\begin{aligned} \dot{V} &= S^T \dot{S} - \tilde{a}_1 \dot{\hat{a}}_1 \\ &= -k_r S^T S + S^T \left[C\Delta f(\cdot) - \frac{\hat{a}_1 \Upsilon_1 S}{\|S\|} \right] - \tilde{a}_1 \dot{\hat{a}}_1 \\ &\le -k_r \|S\|^2 + \tilde{a}_1 (\|S\| \Upsilon_1 - \dot{\hat{a}}_1) = -k_r \|S\|^2 \le 0 \end{aligned}$$

Therefore, it is readily shown the following properties: $S = \dot{E} + \beta E \in L_\infty \cap L_2$ and $\tilde{a} \in L_\infty$. Therefore, with that, we have $E \in L_\infty \cap L_2$, $\dot{E} \in L_\infty \cap L_2$ and $E \in L_\infty$. Also we can show that $\ddot{E} \in L_\infty$, therefore by Barbalat lemma [15], we conclude that *E*, (thus e_x, e_y and e_h) converges to zero as time increases, which completes the proof.

Note that if *G* and *N* are not available, the above control scheme needs to be modified accordingly. To this end, we make the following important observations on *C* and *N*.

Observation 1: For leading a UAV maneuvering with bounded acceleration, there exist two constants c_1 and c_2 *such that*

$$\|N(.)\| \le c_1 |V_l \dot{\psi}_l| + c_2 |\dot{\psi}_w| \left\| \begin{bmatrix} V_w \\ \dot{\psi}_w \\ \dot{h}_w \end{bmatrix} \right\| \tag{32}$$

Proof:

For bounded acceleration maneuvering, $\dot{V}_l$ and $\ddot{h}_l$ are bounded, therefore

$$\|N(.)\| \le c_1 |V_l \dot{\psi}_l| + \|\dot{C}\| \left\| \begin{bmatrix} V_w \\ \dot{\psi}_w \\ \dot{h}_w \end{bmatrix} \right\|$$

Note that

$$\dot{C} = \dot{\psi}_w \begin{bmatrix} -\cos\psi_w & x_d \sin\psi_w + y_d \cos\psi_w & 0 \\ \sin\psi_w & -y_d \sin\psi_w + x_d \cos\psi_w & 0 \\ 0 & 0 & 0 \end{bmatrix}$$

where x_d and y_d are given separation constants, it is seen that $\|\dot{C}\| \le c_2 |\dot{\psi}_w|$ and c_2 is some constant, which leads to (32) readily.

Observation 2: For fully a controllable vehicle, (i.e., $g_v(.) \ne 0,\ g_\psi(.) \ne 0,\ g_h(.) \ne 0\ \ \forall t \ge 0$ *, without loss of generality,* $g_v(.) > 0,\ g_\psi(.) > 0,\ g_h(.) > 0$ *is considered here), the matrix* (CGC^T) *is symmetric and positive definite.*

Proof:

In view of the fact that *C* is invertible and *G* is diagonal and positive, the result can be shown easily.

We are ready to present the second robust adaptive control scheme.

Theorem 2: Consider the transformed error dynamics (23), where the only available information is that control gains $g_v(.) > 0,\ g_\psi(.) > 0,\ g_h(.) > 0$ and the lumped uncertain vector satisfies (26). If the following robust adaptive control scheme is applied, then stable close formation of multi-UAVs is ensured,

$$\begin{bmatrix} u_v \\ u_\psi \\ u_h \end{bmatrix} = -C^T (k_r + k_a) S \tag{33}$$

where *S* is defined as before and

$$k_r > 0,\ k_a = \frac{\hat{a}_2 \Upsilon_2}{\|S\|} \tag{34}$$

with $\dot{\hat{a}}_2 = \|S\| \Upsilon_2$ and

$$\Upsilon_2 = \beta \|\dot{E}\| + \|C\| \sum_{i=1}^{m} \xi_{fi} + |V_l \dot{\psi}_l| + |\dot{\psi}_w| \left\| \begin{bmatrix} V_w \\ \dot{\psi}_w \\ \dot{h}_w \end{bmatrix} \right\| \tag{35}$$

Proof: Let

$$\Delta F(\cdot) = N + C \begin{bmatrix} \Delta f_v \\ \Delta f_\psi \\ \Delta f_h \end{bmatrix} + \beta \dot{E}$$

It can be shown that

$$\begin{aligned} \|\Delta F\| &\le \|N\| + \|C\| \sum_{i=1}^{m} b_i \xi_{fi} + \beta \|\dot{E}\| \\ &\le \max(c_1, c_2) \left[|V_l \dot{\psi}_l| + |\dot{\psi}_w| \left\| \begin{bmatrix} V_w \\ \dot{\psi}_w \\ \dot{h}_w \end{bmatrix} \right\| \right] \\ &\quad + \max(b_1,...,b_m) \sum_{i=1}^{m} \xi_{fi} + \beta \|\dot{E}\| \le a_2 \Upsilon_2 \end{aligned}$$

where $a_2 = \max\{c_1, c_2, b_1, ..., b_m, 1\}$ is defined as in (35). Therefore we can show that the control scheme (32) leads to With the control scheme (25), it is seen that

$$\dot{S} = -k_r (CGC^T) S - (CGC^T) \frac{\mathrm{S}}{\|\mathrm{S}\|} \hat{a}_2 \Upsilon_2 + \Delta F(\cdot) \qquad (36)$$

Consider the Lyapunov function candidate

$$V = \frac{1}{2} S^T S + \frac{1}{2\lambda_{\min}} \tilde{a}_2^{\,2} \qquad (37)$$

where $\tilde{a}_2 = a_2 - \lambda_{\min} \hat{a}_2$ and $\lambda_{\min} > 0$ is the minimum eigenvalue of matrix (CGC^T). It follows from (36)-(37) that

$$\begin{aligned} \dot{V} &= S^T \dot{S} - \tilde{a}_2 \dot{\hat{a}}_2 \\ &= -k_r S^T (CGC^T) S + S^T \left[\Delta F(\cdot) - (CGC^T) \frac{\mathrm{S}\hat{a}_2 \Upsilon}{\|\mathrm{S}\|} \right] - \tilde{a}_2 \dot{\hat{a}}_2 \end{aligned}$$

Using the fact that

$$\lambda_{\min} \|S\|^2 \le S^T (CGC^T) S \le \lambda_{\max} \|S\|^2$$

we get

$$\begin{aligned} \dot{V} &\le -k_r \lambda_{\min} \|S\|^2 - \lambda_{\min} \|S\| \hat{a}_2 \Upsilon_2 + \|S\| \Upsilon_2 a_2 - \tilde{a}_2 \dot{\hat{a}}_2 \\ &= -k_r \lambda_{\min} \|S\|^2 + \|S\| \Upsilon_2 \tilde{a}_2 - \tilde{a}_2 \dot{\hat{a}}_2 \\ &= -k_r \lambda_{\min} \|S\|^2 + \tilde{a}_2 (\|S\| \Upsilon_2 - \dot{\hat{a}}_2) \\ &= -k_r \lambda_{\min} \|S\|^2 \le 0 \end{aligned}$$

The result is established using the argument similar to the proof of Theorem 1.

Remarks

1. The overall control scheme is illustrated in Figure 3. The proposed control scheme is fairly simple in structure and demands no detail information on flight dynamics of the vehicle. This implies that the control scheme can be easily implemented without involving complicated on-line computations, re-design or re-program.
2. Since the control algorithms does not involve $\lambda_{\min}$, there is no need to analytically calculate such parameter in control design.

IV. Simulation Verification

As the verification, we conduct computer simulation on three UAVs in close formation. The flight characteristics and simulation parameters for Leader UAV, Wingman A and B are shown in Table III. The initial relative flying positions for Wingman A and Wingman B are $[100 \quad 60 \quad 5{,}000]$ (ft) and $[90 \quad -50 \quad -29{,}000]$ (ft), respectively.

The vortex effect is considered as given in Proud et al [2]. Under varying flight conditions the precise value of dynamic pressure $\bar{q}$ and the lift, drag and side-wash coefficients are unavailable, which, together with the nonlinear lumped uncertainties, are treated completely unknown in the simulation.

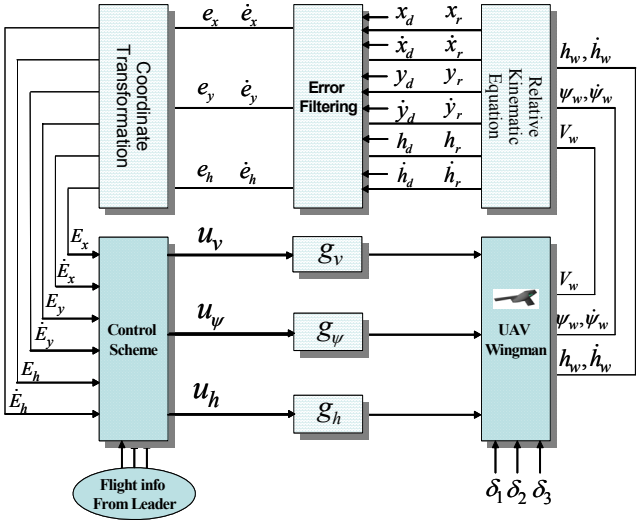

Fig. 3. Control Scheme Diagram

Simulations on vertical, horizontal and Δ -shaped formation were conducted. Only partial results are presented here due to pager limit. The simulation results are presented in Figure 4-6, where Figure 4 is the separation distance trajectory tracking error along lateral (*x*-axis), longitudinal (*y*-axis) and vertical (*h*-axis) direction, respectively, which shows the precise tracking performance. The heading velocity and heading angle trajectory tracking are shown in Figure 5. The control signal for u_v, u_ψ and u_h are depicted in Figure 6. As can be seen, the proposed control scheme works very well in maintaining the desired formation under the effect of vortex. The control action is bounded and smooth.

TABLE III
Aircraft Characteristic Values

Parameter	Value	Unit
Velocity time constant	5	secs
Heading time constant	0.75	secs
Dynamic Pressure	155.8	lb/ft^2
Formation Heading Velocity	825	ft/s
Wing Area	300	ft^2
Wing Span	30	ft
Mass	776.4	lb

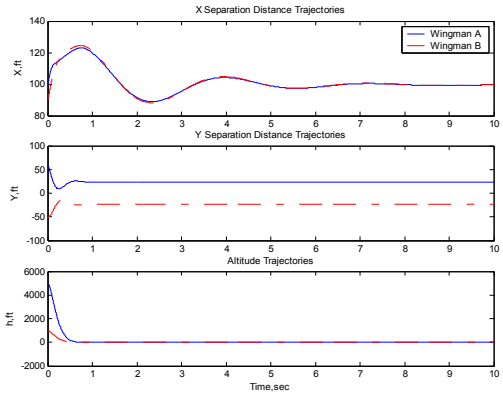

Fig. 4. Separation distance tracking

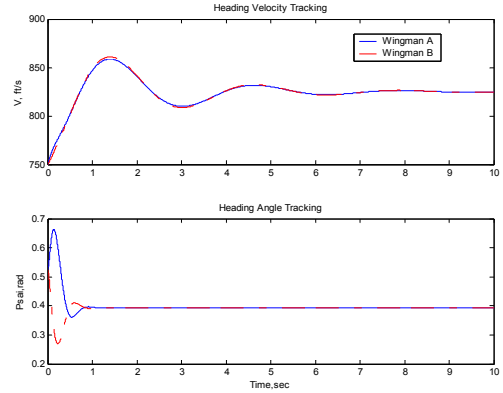

Fig. 5. Heading velocity and heading angle tracking

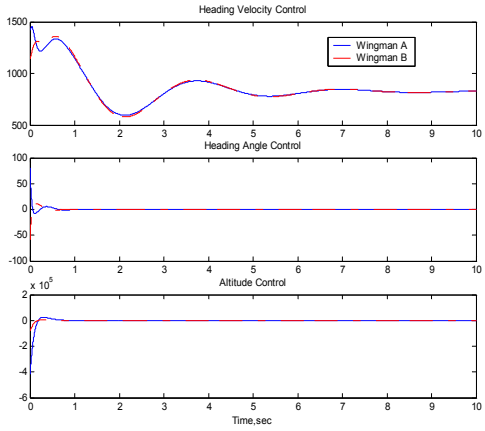

Fig.6. Control signal of heading velocity, heading angle and altitude

V. Conclusion

The problem of close formation control of multi-UAVs is investigated in this paper. A new robust and adaptive control scheme is proposed, which is shown to be capable of dealing with the system nonlinearities and external disturbances due to close formation. In deriving the control scheme, general dynamic flight model reflecting vortex effects is considered. Simulation on three UAVs (one leader flowing with two wingman) was conducted. The results demonstrate that the proposed control scheme is adaptive and robust over wide varying flight conditions.

References

[1] W. Blake and D. Multhopp, Design, Performance and Modeling Consideration for Close Formation Flight. *AIAA Guidance, Navigation and Control Conference*, Boston, MA, July 1998.

[2] A. W. Proud, M. Pachter, and J. J. D'Azzo: Close Formation Flight Control; AIAA Guidance, Navigation, and Control Conference, Vol. 2, pp. 1231–1246 (1999)

[3] L. E. Buzogany, M. Pachter, J. J. D'Azzo: Automated Control of Aircraft in Formation Flight; AIAA Guidance, Navigation, and Control Conference, Part. 3, pp. 1349–1370 (1993)

[4] R.Fierro, C.Belta, J.P. Desai, and V. Kumar: "On Controlling Aircraft Formation" in Proc. 40th IEEE Conf on Decision and Control, Orlando, FL, December 2001,pp 1065-1070

[5] F.Giulitti, L. Pollini, and M. Innocenti, "Autonomous formation flight". IEEE Control System, vol 20, no.6,pp34-44, 2000

[6] V. J. Jongusuk, T. Mita, Y. Masuko. "Tracking Control of UAV in 3D Space - Toward Formation Control". *The 30th Symposium on System Theory*, Oita, Japan, 2001.

[7] V. P. Reyna, M. Pachter, J. J. D'Azzo. "Formation Flight Control Automation". AIAA Guidance, Navigation, and Control Conference, Part. 3, pp. 1379–1404 (1994)

[8] A. Richards, J. Bellingham, M. Tillerson, and J. P. How. "Coordination and Control of Multiple UAVs". *AIAA Guidance, Navigation, and Control Conference*, Monterey, CA, 2002.

[9] J. D. Wolfe, D. F. Chichka, and J. L. Speyer. "Decentralized controllers for unmanned aerial vehicle formation flight". *AIAA Guidance Navigation and Control Conference*, San Diego, CA, July, 1996.

[10] S. N. Singh. "Adaptive Feedback Linearization Nonlinear Close Formation Control of UAVs". Proceedings of American Control Conference, pp. 854–858 (2000)

[11] Corey Schumacher and Sahjendra N. Singh. "Nonlinear Control of Multiple UAVs in Close-Coupled Formation Flight", AIAA Guidance, Navigation, and Control Conference, 2000, Denver, CO, August, Paper no. AIAA~2000-4373.

[12] Y. D. Song, Y. Li, M. Bikdash and T. Dong . "Cooperative Control of Multiple UAVs in Close Formation Flight ViaSmooth Robust and Adaptive Approach". 4th International Conference onCooperative Control and Optimization. Destin, FL, November 19–21, 2003

[13] Snell, S. A. "Decoupling Control Design with Applications to Flight," Journal of Guidance, Control, and Dynamics, Vol. 21, No. 4, July-August 1998, pp. 647-655.

[14] Reigelsperger W. C., Banda S. S. and Lemaster D. P., Application of Multivariable Control Theory to Aircraft Control Laws, WL-TR-96-3099, Wright Laboratory, Wright-Patterson AFB, Ohio, May 1996.

[15] J. J. Slotine and W. Li: Applied Nonlinear Control, Prentice-Hall, Inc., 1991.